LASER & PHOTONICS REVIEWS
www.lpr-journal.org

Efficient Spectral Broadening and Few-Cycle Pulse Generation with Multiple Thin Liquid Films

Jiacheng Huang, Xiang Lu, Feilong Hu, Yu Deng, Jie Long, Jiajun Tang, Lixin He, Qingbin Zhang, Pengfei Lan, and Peixiang Lu*

High-energy, few-cycle laser pulses are essential for numerous applications in the fields of ultrafast optics and strong-field physics, due to their ultrafast temporal resolution and high peak intensity. In this work, different from the traditional hollow-core fibers and multiple thin solid plates, the generation of an octave-spanning supercontinuum broadening is demonstrated by utilizing multiple ultrathin liquid films (MTLFs) as the nonlinear media. The continuum covers a range from 380 to 1050 nm, corresponding to a Fourier transform limit pulse width of 2.5 fs when 35 fs Ti: sapphire laser pulse is applied on the MTLFs. The output pulses are compressed to 3.9 fs by employing chirped mirrors. Furthermore, a continuous high-order harmonic spectrum up to the 33rd order is realized by subjecting the compressed laser pulses to interact with Kr gas. The utilization of flowing liquid films eliminates permanent optical damage and enables wider and stronger spectrum broadening. Therefore, this MTLFs scheme provides new solutions for the generation of highly efficient supercontinuum and nonlinear pulse compression, with potential applications in the fields of strong-field physics and attosecond science.

1. Introduction

Intense ultrafast lasers with few-cycle pulse widths play an essential role in the fields of strong-field physics, ultrafast optics, and attosecond science.[1–7] Such ultrafast pulses can be achieved through nonlinear post-compression techniques, which rely on the interplay between supercontinuum generation (SCG) and compensation of dispersion.[8–10]

The SCG can be achieved by self-phase modulation (SPM), self-steepening, and ionization between intense laser pulses and nonlinear medium.[11–14] Extensive experimental and theoretical research has been conducted over several decades based on various nonlinear media, including gases and transparent solids.[15–17] For many years, gas-filled hollow-core fibers (HCFs) pulse compressors have garnered considerable attention for their high beam quality and high compression factors.[18,19] However, the practical utility of HCFs is constrained by the limitations on the incident energy and the strong nonlinear effects in the fibers, arising from the inherent constraints on the waveguide structures and the small core diameters. Pointing-stabilization setups are required for alignment and the coupling efficiency of fibers is usually low.[20] The scheme using multiple thin solid plates (MTSPs) has gained significant interest due to its simplicity, compactness, flexibility, and free-space geometric characteristics.[21–26] Notably, the generation of quasi-stationary spatial solitons in periodic-layered Kerr media has emerged recently as a promising scheme to enhance the nonlinear light–matter interaction and suppress the spatial and temporal losses.[27–29] More recently, a multi-pass cell (MPC) scheme has also been reported for the spectral homogeneity across the beam profile.[30–32] The threshold of self-focusing in solid medium is typically on the order of a few MW. Whereas in inert gas, it is much higher (≈10 GW).[11] The spectrum range of MPC may be narrower than that of MTSPs and HCFs, and the relatively low compression ratio usually requires two-stage nonlinear compression for producing few-cycle pulses.[33–35]

Due to the higher nonlinear susceptibility and larger molecular density compared to gases,[11,36] we expect physical mechanisms would be magnified in the liquid medium.[37,38] However, to our knowledge, no research has been conducted on the nonlinear compression of few-cycle pulses with liquid medium. Although supercontinuum can be obtained in condensed liquid, it is still restricted to the input energy limitation and optical loss caused by self-focusing and filamentation.[39,40] Studies show that spectrum broadening precedes pulse splitting or optical breakdown.[41] To address these challenges, we propose controlling the liquid's thickness to obtain multiple thin liquid films (MTLFs). This arrangement ensures that laser pulses solely experience spectral broadening due to self-phase modulation in the

J. Huang, X. Lu, F. Hu, Y. Deng, J. Long, J. Tang, L. He, Q. Zhang, P. Lan, P. Lu
Wuhan National Laboratory for Optoelectronics and School of Physics
Huazhong University of Science and Technology
Wuhan 430074, China
E-mail: pengfeilan@hust.edu.cn
L. He, Q. Zhang, P. Lan, P. Lu
Optical Valley Laboratory
Hubei 430074, China
P. Lan, P. Lu
Hubei Optical Fundamental Research Center
Wuhan 430074, China

The ORCID identification number(s) for the author(s) of this article can be found under https://doi.org/10.1002/lpor.202301191

DOI: 10.1002/lpor.202301191

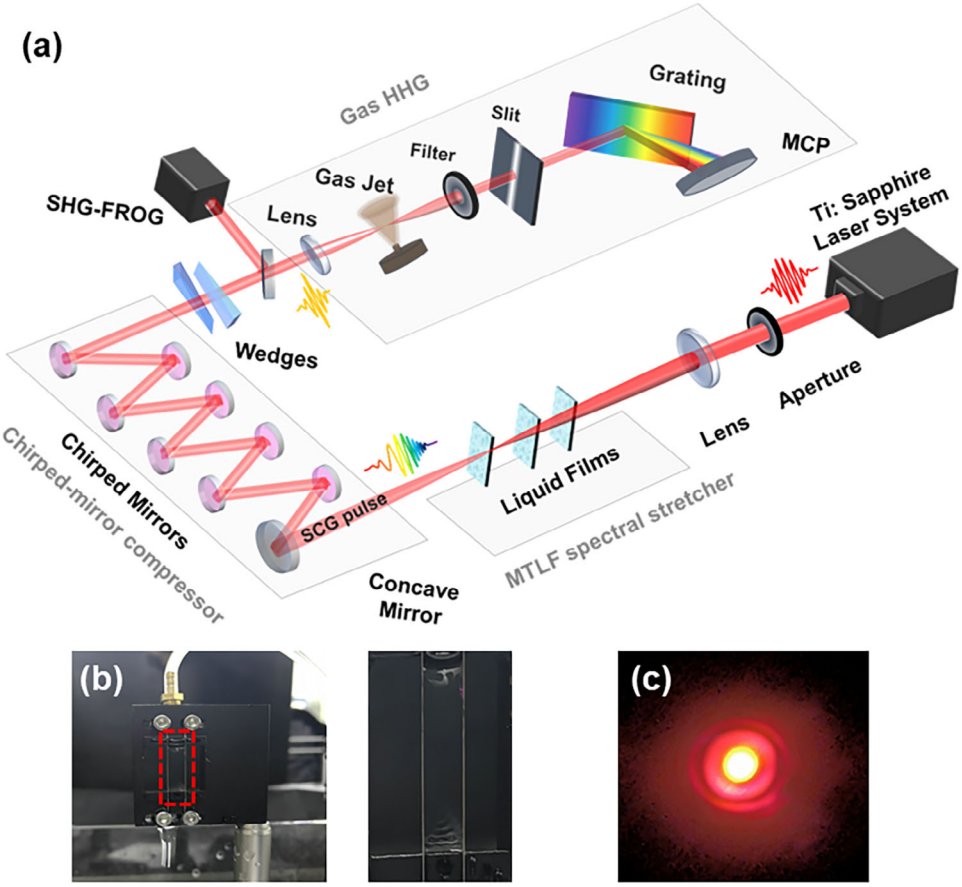

Figure 1. a) Schematic of the experimental setup for few-cycle pulses compression and HHG. The experiment of gas HHG is carried out under vacuum conditions. b) The gravity-driven ultrathin liquid film workpiece. c) The beam profile is collected on flat paper and imaged on a camera.

ultrathin films. When compared to solid or gas media, the MTLFs scheme offers several potential advantages. First, there is no permanent optical damage in the flowing liquid, allowing for high-intensity laser input. Liquid degradation or surface damage could be avoided by the continuous refresh of liquid.[42] Additionally, the fluidity of liquid ensures a fresh area for each pulse. Third, the nonlinear refractive index of water (5.7×10^{-20} m^2 W^{-1}) is much higher than fused silica (FS),[11,44] theoretically leading to SCG with a wider spectral range and stronger intensity. Based on the above consideration, multiple ultrathin water films show promise as a better spectral broadening scheme, potentially supplanting the traditional gas-filled HCFs and solid thin plates.

In this paper, we demonstrate the generation of sub-4-fs few-cycle laser pulses by octave-spanning supercontinuum based on the multiple thin water films scheme. The obtained supercontinuum covers from 380 to 1050 nm with an efficiency of up to 86.7%. After dispersion compensation by chirped mirrors, the chirped pulses are compressed from 35 to 3.9 fs successfully. The quality of the compressed pulses is further confirmed by high-harmonic generation. A continuous high-order harmonic spectrum up to the 33rd order is achieved based on the compressed few-cycle laser pulses.

2. Nonlinear Compression Experiment

2.1. The Generation of Supercontinuum

First, we investigate the supercontinuum generation using MTLFs. The schematic of our experimental set-up is shown in **Figure 1**. A commercial 800 nm Ti: sapphire laser system (Astrella-USP-1K, Coherent, Inc.) is employed as the pump source, which delivers 35 fs pulses at a repetition rate of 1 kHz. An iris aperture is used to reduce the beam size to 6 mm for a larger Rayleigh range at the focus. Through the convex lens of f = 2000 mm, the Rayleigh range is measured to be 16.1 cm with the peak power of the focused beam at ≈17 GW (pulse energy 0.6 mJ). Multiple ultrathin wire-guided free-flowing liquid films are employed in our experiment, as depicted in Figure 1b. Benefiting from the balance between high surface tension and the gravity of the liquid, a flow guided by two Ni-80 wires with a diameter of 200 μm forms a thin liquid film.[44] We first choose water as the broadened liquid medium for it is cost-effective and easily available. Its transmission efficiency of up to 99% in the visible band ensures the high-efficiency output of SCG.[43]

Laser pulses would only experience spectral broadening due to SPM, and exit the film before filamentation and optical damage occur. After passing through the film, the beam gets focused

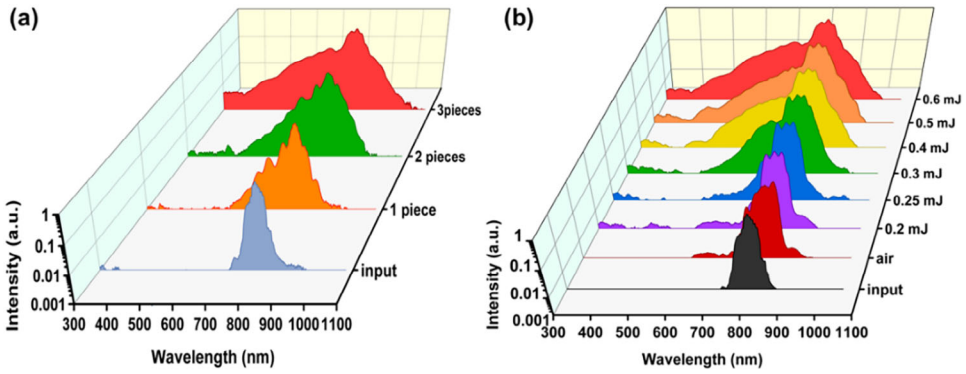

Figure 2. a) Experimentally measured spectra after each water film at the incident energy of 0.6 mJ. b) Broadened spectra with three pieces of water films under different incident pulse energies.

in the air and then diverges. The divergent beam would be refocused by the self-focusing effect inside the next film. This method can circumvent the filamentation and optical breakdown, allowing for the enhancement of the nonlinear Kerr interaction inside the liquid.

By carefully optimizing and adjusting the positions of films near the focus, we achieve the optimal conditions for SCG with three water films. The first water film is placed ≈100 mm in front of the focal point, and the spacings between the films are 118 and 50 mm, respectively. It is worth noting that the thickness of the water films can be easily adjusted by controlling the water flow rate and the spacing between two wires, which will provide flexibility in tuning the nonlinear phase shift accumulated in the water films. To measure the nonlinear broadening spectrum, we utilize a Charge Coupled Device (CCD) optical spectrometer (AvaSpec-2048FT-SPU) and position it 60 cm downstream from the focus.

The far-field beam profile after spectrum broadening is captured on a flat piece of white paper and imaged onto a camera, as depicted in Figure 1c. The beam spot represents a high-quality transverse mode with a zeroth-order Bessel function, which is similar to the phenomenon observed in the scheme of FS plates.[11] In general, the white light beam generated during filament in gases and condensed media would consist of a bright round central zone surrounded by conical emission.[45] An iris aperture is employed to block outer diffraction rings before recollimation. The energy proportion of the center spot is 79.7%, much higher than that of HCFs systems (≈50%).[19] The beam instability caused by the generation of liquid films can be further optimized by improving the liquid film workpiece.

The spectrum evolution of fundamental femtosecond pulses after the MTLFs is depicted in **Figure 2a**. The pulse spectrum broadens incrementally after passing through each water film. After the first water film, the spectrum expands from its initial range of 740–860 to 580–960 nm. As the second film is introduced, further spectral broadening occurs, resulting in a range of 480–985 nm. In the first two films, the broadened spectra exhibit symmetrical expansion on both the red and blue sides, which is in accordance with the process of SPM.[46] However, the more pronounced blue extension is observed after propagating through the last water film due to the self-steepening and ionization effects, as demonstrated previously in the FS plates broadening scheme.[22] Three water films are employed for maximum broadening, no significant further spectral broadening effect is observed when adding more water films. Ultimately, at an intensity level of −30 dB, the final broadened spectrum covers a range of 380–1050 nm, corresponding to the Fourier Transform Limit (FTL) pulse duration of 2.5 fs. The supercontinuum output energy reaches 0.52 mJ with an efficiency of 86.7%, generally much higher than that of HCF. The total energy loss of ≈10% through the three water films can be attributed to multiphoton absorption and ionization in water.[47] Additionally, diffuse reflection caused by the non-smooth surface of water films also contributes to certain energy loss.

The applicable range of input laser energy in our MTLFs scheme is also characterized. By utilizing a combination of a half-waveplate (HWP) and a polarizer, we continuously reduce the incident pulse energy from 0.6 to 0.2 mJ at 0.1 mJ intervals. The input beam waist size and the position of water films remain unchanged. Thus, the incident intensity on the water films for SCG solely depends on the incident pulse energy. The obtained broadening spectra under different input energies are shown in Figure 2b. As the incident laser energy decreases, the range of the broadened spectrum reduces significantly. When the input energy drops below 0.2 mJ, no considerable spectral broadening occurs. It indicates that the nonlinear intensity is too weak to achieve SPM in the water films under this circumstance. In the case of low-energy laser input, the focusing lens with a smaller focal length can be employed to obtain sufficiently high intensity for SCG.

Additionally, we conduct the supercontinuum generation with MTLFs under high-energy laser input. 1 mJ energy and 1 kHz repetition rate laser pulses are injected into the thin water films. In this case, the intense average power will lead to the evaporation of the thin water film and the filamentation in water under the conditions of the previous experimental setup. To address this issue, adjustments are made to optimize supercontinuum generation by modifying the positions and spacings between the water films. Compared to the relatively low-intensity input, the spectral broadening through air is more pronounced with 1 mJ energy input. As depicted in Figure 2b, the final spectral broadening covers a range from 420 to 1000 nm at the −30 dB bandwidth. Despite the difference in incident energies, the spectral configurations are similar in both cases. Furthermore, after passing

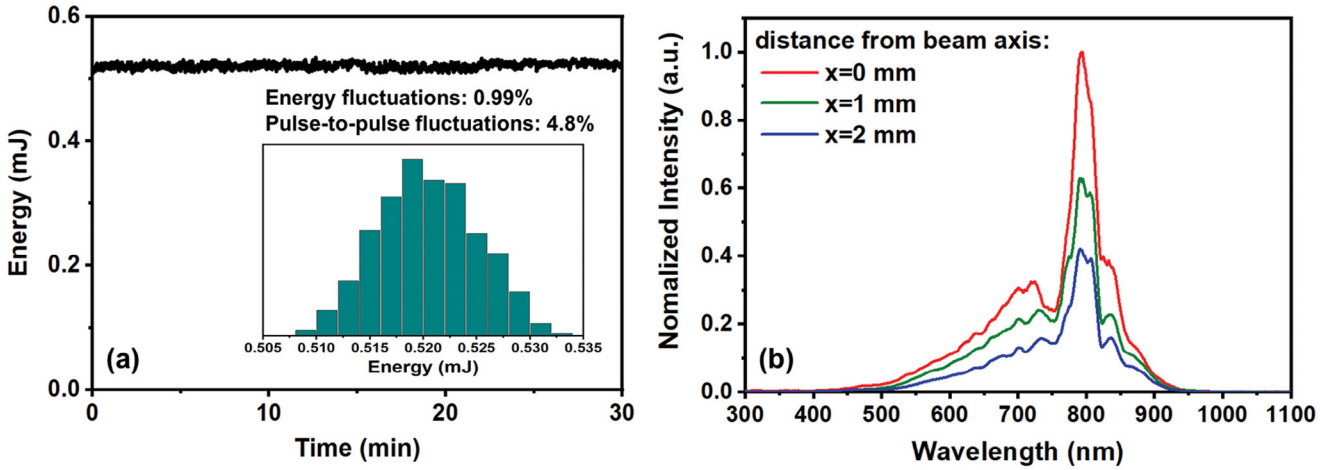

Figure 3. a) The long-term energy stability of the supercontinuum output. b) Characterization of the homogeneity of spectra across the beam profile.

through three water films, the output energy is measured to be 0.84 mJ with a conversion efficiency of 84%. As for much higher pulse energy input, a focusing lens with a larger focal length is required. It is necessary to maintain relatively constant nonlinear intensity on the liquid films for effective SCG. The large range of permissible pulse energies input of our MTLFs setup makes it a promising platform for various SCG and nonlinear compression applications.

Figure 3a illustrates the long-term energy stability of the supercontinuum output before the chirped-mirror compressor. The RMS fluctuation of the pulse energy over 30 min is quantified at 0.99% with a mean average energy of 0.52 mJ when the input pulse energy is 0.6 mJ, representing the sustained stability of the MTLFs system. Meanwhile, the measured energy stability of the input pulses is ≈0.3% and the flowing liquid also causes certain influence. The inset in Figure 3a presents a histogram of the energy distributions and the pulse-to-pulse (PTP) fluctuations is 4.8%.

In general, the inhomogeneous spectral broadening across the beam profiles can be avoided in the MTLFs scheme by restricting a small nonlinear phase in each liquid film. To characterize the homogeneity of the spectral broadening, a multimode fiber with an FC/PC tip is scanned across the profile in steps of 1 mm along the *x*-axis. As spectra along the *x*-axis are depicted in Figure 3b, the widths of the spectra do not vary much, and also the centroid of the spatial spectra. From the above power stability and the spatial-spectral distribution of the broadened beam, the supercontinuum beam output obtained by our MTLFs has relatively good stability and spatial homogeneity.

Under the current experimental parameters, we have not observed significant effects of liquid film evaporation on the spectrum-broadening experiment. To evaluate the thermal effects, we employ the simple formula for temperature change induced by energy absorption in a flowing water film, i.e., $\Delta T = \Delta Q/(m \times C)$, where ΔQ denotes the absorbed heat energy, m is the mass of the flowing water, and C denotes the heat capacity. Under full load 6 W power input, the heat energy absorbed by water is ≈0.06 W, considering the absorption of water at 800 nm wavelength. By incorporating the flow velocity of the water film into our analysis, the calculation indicates that the temperature

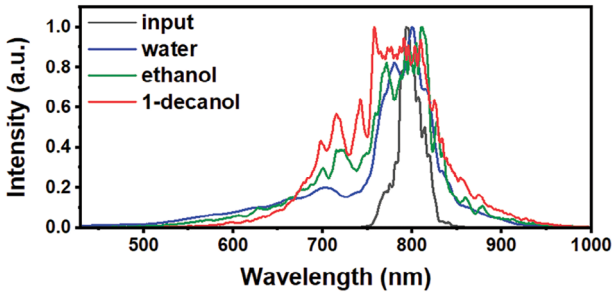

Figure 4. The comparison of SCG between water, ethanol, and 1-decanol.

rise in the flowing water film is ≈0.1 °C. Even with an average power input of 100 W, the temperature increment is merely 1.7 °C. Such a small temperature change does not result in obvious evaporation and will not influence our experiment. Moreover, considering the dynamic flow of the water, the heat dissipation is continuous, significantly mitigating the thermal impact on the experiment.

Next, we investigate the influence of the nonlinear Kerr index coefficient n_2 on the broadening. To this end, we choose two more alcohols with higher n_2 value as nonlinear media, ethanol and 1-decanol, whose nonlinear Kerr index are 7.7×10^{-20} and 11×10^{-20} m^2 W^{-1}, respectively.[47] Under the identical input laser parameters and experimental setup, the broadened spectra can be achieved by using three 200 μm liquid films similar to the water-thin films. For comparison, we show the broadened spectral with water, ethanol, and 1-decanol in **Figure** 4. When the spectral intensity is above −10 dB (in the range of 650–850 nm), the employing of ethanol and 1-decanol has been observed to induce a significantly stronger and wider broadening spectrum compared to water. Notably, the spectral broadening intensity exhibited by 1-decanol films is threefold that of water films near 700 nm. At wavelengths below 650 nm, water demonstrates the most extensive blue broadening conversely; however, the intensity of this spectral component remains less than −10 dB. Beyond 850 nm, the red broadening manifested in alcohols is more extensive than that in water.

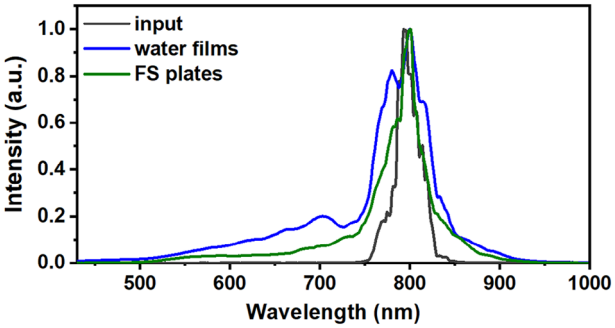

Figure 5. The comparison of SCG between MTLFs and FS plates scheme.

Based on the experimental results involving three liquids with varying nonlinear Kerr index coefficients, it was observed that the intensity of the supercontinuum generated in ethanol and 1-decanol significantly surpasses that obtained in water, as shown in Figure 4. It is worth noting that the spectral components above 650 nm exhibit a more pronounced broadening effect with two alcohols. And with the increase of the nonlinear coefficient index n_2, the range of the red broadening also increases. These enhancements benefit from the more significant nonlinear SPM effect induced by a higher n_2 value. Nevertheless, water facilitates the shorter cut-off wavelength of blue broadening below −10 dB intensity, aligning with the multiphoton ionization and bandgap dependence theories in Ref.[36]

We also conduct a comparison experiment using traditional solid fused silica (FS) plates as the nonlinear media for SCG. Under similar laser input conditions, the supercontinuum in the multiple FS thin plates scheme expands from 450 to 980 nm. The total thickness of the six pieces of FS plates is 600 μm. As depicted in **Figure 5**, it is evident that the spectrum achieved with the MTLFs setup exhibits wider range and higher intensity, indicating the stronger nonlinear interaction in the water films. Moreover, the intensity of the broadened spectrum below 500 nm based on water films is even ten times higher than that achieved with FS plates, although both water and fused silica possess bandgaps of 7.5 eV.[47] Note that the broadening effect with 1-decanol is much stronger than that of fused silica (see Figures 4,5). These results not only validate the feasibility of utilizing ultrathin water films for SCG, but also highlight their superiority over traditional FS plates in terms of spectral broadening and intensity enhancement, showing great potential for subsequent nonlinear pulse compression.

To gain further insight into the experimental results of SCG, we conduct numerical solutions of the generalized nonlinear Schrodinger equation (NLSE) to investigate the pulse propagation [48] (see Supporting Information). The simulated spectral configuration closely agrees with the experimental results. The Kerr nonlinear optical responses, including SPM and the self-steepening, act jointly with the dispersion effect and play a major role in spectral broadening. The influence of the nonlinear refractive index n_2 of the medium on the spectral broadening is verified theoretically. The spectra with a wider range and higher intensity obtained in our MTLFs scheme are affected by the larger nonlinear refractive index n_2. The theoretical results indicate that the compressed pulse duration would be shorter under a relatively large nonlinear refractive index n_2 and low group velocity dispersion β_2, which is in agreement with the Ref.[49] Additionally, the effect of the thickness of water films on broadening and self-focusing has been investigated (see Figure S2, Supporting Information). The increasing self-focusing effect in an excessively thick medium leads to the formation of filaments and eventual beam degradation and collapse.

2.2. The Pulse Compression

To compress the pulse duration, four pairs of chirped mirrors (Ultrafast Innovations) with 450–1000 nm bandwidth and GDD = −40 fs^2 are utilized to compensate for the chirp of the output pulses. Additionally, a pair of wedges is incorporated to finely tune the dispersion. Note that, considering the cost-efficiency, accessibility, and broader spectral expansion, we only adopt water as the nonlinear medium in the subsequent experiments. The efficiency of the output pulse energy, measured after the chirped mirrors, is ≈91.4%. Moreover, the center spot of the output beam contains an energy of ≈0.37 mJ.

A homemade scanning second-harmonic generation frequency-resolved optical gating (SHG-FROG) measurement is utilized to record the temporal and spectral characterizations of the compressed pulses. **Figure 6**a,b represent the measured and retrieved FROG traces of the compressed pulses, respectively, with the retrieved error of 0.005. Figure 6c illustrates the reconstructed temporal profile of pulse duration (blue solid) and phase (orange solid). The duration of pulses is measured to be 3.9 fs by FROG, corresponding to 1.6 FTL (FTL = 2.5 fs) of the measured spectrum. And the pulse compression factor K_c is ≈10. The difference in pulses characteristics may be attributed to the bandwidth limitations of the chirped mirrors, as some spectral components are not fully compensated for dispersion. As shown in Figure 6d, the retrieved spectrum in the blue line agrees well with the actual spectrum measured by the spectrometer (shaded area). The spectral phase is relatively flat in the spectral range of 600–1000 nm, suggesting the effect of SPM plays a dominant role in this spectral broadening region and dispersion has been effectively compensated in the experiment. However, below 600 nm, the spectral phase exhibits modulation due to possible contributions from the self-steepening effect and ionization.

2.3. HHG Experiment

To further demonstrate the quality of the compressed pulses, we carry out the high-order harmonic generation experiment by interacting with Kr gas after compressing the supercontinuum. After the chirped mirrors compressor stage, certain loss is induced by multiple reflections on the silver mirrors and the vacuum window. The compressed few-cycle pulses laser with the energy of 0.26 mJ is focused onto a gas target inside a vacuum chamber using a concave mirror with a focal length of 150 mm. Note that a certain amount of dispersion would be introduced during propagation through long-distance air and the vacuum chamber window. The generated high-order harmonics are detected by a homemade flat-field soft X-ray spectrometer, which consists of a 0.2 mm-wide, 15 mm-height entrance slit, a flat-field grating (1200 grooves mm^{-1}), and a microchannel plate backed with a

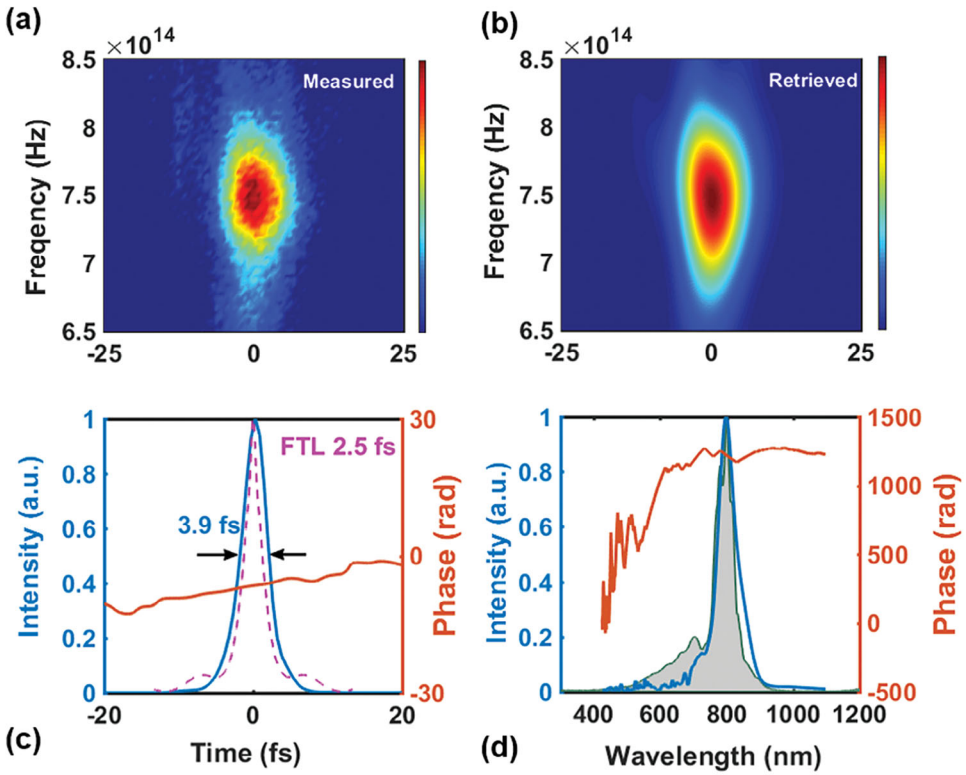

Figure 6. Characterization of the 3.9 fs few-cycle pulses compressed from the supercontinuum by homemade SHG-FROG. a,b) Measured and retrieved FROG traces. c) Retrieved pulse envelop (solid blue line), FTL pulse of 2.5 fs (dashed line), and temporal phase (solid orange line). d) Retrieved spectrum (solid blue line), the spectrum measured by the spectrometer (shaded region), and the spectral phase (solid orange line).

phosphor screen.[50] The spectrally resolved images are recorded using a CCD camera.

As shown in **Figure** 7, the cut-off region of the high-order harmonic spectrum is continuous and smooth. The signal of the 33rd harmonic with photon energy up to 51 eV is observed in the generated supercontinuum, corresponding to an approximate peak intensity of 1.8×10^{14} W cm^{-2} in the interaction region. In contrast to the compressed few-cycle pulses, we also inject the uncompressed pulses (35 fs in the full-width-at half-maximum) into the chamber. The corresponding odd harmonics appear discrete in the spectrum and the peaks are noticeably sharper. More importantly, one can see that the strongest harmonic is ≈ the 17th order in the multi-cycle laser pulse and the strongest harmonic is extended to the 25th harmonic in the few-cycle pulse. Such an extension is notable considering that the cutoff energy is ≈33rd harmonic. Moreover, the observed supercontinuum signal in the 33rd harmonic demonstrates the potential for follow-up attosecond pulse generation and attosecond science applications.

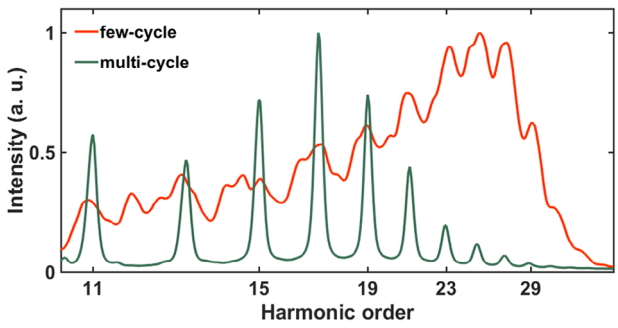

Figure 7. Experimentally measured high-order harmonic spectra generated in krypton driven by compressed few-cycle pulses (red) and uncompressed multi-cycle pulses (green).

3. Conclusion

In this work, we demonstrate the generation of an octave-spanning supercontinuum based on multiple ultrathin liquid films. The widest broadening spectrum achieved using water covers a wide range from 380 to 1050 nm with an efficiency of 86.7%. Few-cycle 3.9 fs laser pulses are achieved successfully after dispersion compensation by chirped mirrors. The high quality of the compressed pulses is further confirmed by the generation of a continuous high-harmonic spectrum up to the 33rd order. This MTLFs scheme provides valuable solutions for SCG covering from ultraviolet to near-infrared and nonlinear pulse compression with few-cycle durations. Furthermore, this work has potential applications in the fields of high-order harmonic generation and attosecond pulse generation, contributing to the advancement of ultrafast science and strong-field physics.

Supporting Information

Supporting Information is available from the Wiley Online Library or from the author.

Acknowledgements

The authors thank Xicheng Zhang, and Yiwen E for the helpful discussions on the thin liquid films. Funding. National Key Research and Development Program of China (No.2023YFA1406800), National Nature Science Foundation of China (no.91950202, no.12225406, no.12074136, no.12021004).

Conflict of Interest

The authors declare no conflict of interest.

Data Availability Statement

The data that support the findings of this study are available from the corresponding author upon reasonable request.

Keywords

few-cycle pulse, high-order harmonic generation, multiple thin water films, post compression

Received: November 16, 2023
Revised: August 18, 2024
Published online:

[1] I. Litvinyuk, K. Lee, P. Dooley, D. Rayner, D. Villeneuve, P. Corkum, *Phys. Rev. Lett.* **2003**, *90*, 233003.
[2] E. Goulielmakis, Z. Loh, A. Wirth, R. Santra, N. Rohringer, V. Yakovlev, S. Zherebtsov, T. Pfeifer, A. Azzeer, M. Kling, S. Leone, F. Krauszet, *Nature* **2010**, *466*, 739.
[3] T. Suzuki, S. Minemoto, T. Kanai, H. Sakai, *Phys. Rev. Lett.* **2004**, *92*, 133005.
[4] J. Li, J. Lu, A. Chew, S. Han, J. Li, Y. Wu, H. Wang, S. Ghimire, Z. Chang, *Nat. Commun.* **2020**, *11*, 2748.
[5] M. F. Kling, M. J. Vrakking, *Ann. Rev. Phys. Chem.* **2008**, *59*, 463.
[6] T. Brabec, F. Krausz, *Rev. Mod. Phys.* **2000**, *72*, 545.
[7] F. Krausz, M. Y. Ivanov, *Rev. Mod. Phys.* **2009**, *81*, 163.
[8] M. Nisoli, D. Silvestri, O. Svelto, *Appl. Phys. Lett.* **1996**, *68*, 3793.
[9] T. Nagy, P. Simon, L. Veisz, *Adv. Phys.: X* **2020**, *6*, 1845795.
[10] E. Khazanov, S. Mironov, G. Mourou, *Phys.-Usp.* **2019**, *62*, 1096.
[11] A. Couairon, A. Mysyrowicz, *Phys. Rep.* **2007**, *441*, 47
[12] N. Aközbek, M. Scalora, C. Bowden, S. Chin, *Opt. Commun.* **2001**, *191*, 353.
[13] A. L. Gaeta, *Phys. Rev. Lett.* **2000**, *84*, 3582.
[14] R. R. Alfano, *The Supercontinuum Laser Source: The Ultimate White Light*, Springer, New York **2016**.
[15] M. Wittmann, A. Penzkofer, *Opt. Commun.* **1996**, *126*, 308.
[16] A. Dubietis, G. Tamouauskas, R. Uminas, V. Jukna, A. Couairon, *Lith. J. Phys.* **2017**, *57*, 113.
[17] R. Dorsinville, P. Ho, J. Manassah, R. Alfano, *The Supercontinuum Laser Source*, Springer, New York **2006**.
[18] G. Fan, T. Balciunas, T. Kanai, T. Flöry, G. Andriukaitis, B. E. Schmidt, F. Légaré, A. Baltuška, *Optica* **2016**, *3*, 1308.
[19] V. Cardin, N. Thire, S. Beaulieu, V. Wanie, F. Legare, B. Schmidt, *Appl. Phys. Lett.* **2015**, *107*, 181101.
[20] T. Nagy, S. Hdrich, P. Simon, A. Blumenstein, J. Limpert, *Optica* **2019**, *6*, 1423.
[21] C. Lu, Y. Tsou, H. Chen, B. Chen, Y. Cheng, S. Yang, M. Chen, C. Hsu, A. Kung, *Optica* **2014**, *1*, 400.
[22] P. He, Y. Liu, K. Zhao, H. Teng, X. He, P. Huang, H. Huang, S. Zhong, Y. Jiang, S. Fang, X. Hou, Z. Wei, *Opt. Lett.* **2017**, *42*, 474.
[23] Y. Cheng, C. Lu, Y. Lin, A. Kung, *Opt. Express* **2016**, *24*, 7224.
[24] F. Hu, Q. Zhang, J. Cao, Z. Hong, W. Cao, P. Lu, *Opt. Lett.* **2022**, *47*, 389.
[25] R. Budriunas, D. Kucinskas, A. Varanavicius, *Appl. Phys. B* **2017**, *123*, 212.
[26] X. Xie, Y. Deng, S. Johnson, *High Power Laser Sci. Eng.* **2021**, *9*, e66.
[27] S. Zhang, Z. Fu, B. Zhu, G. Fan, Y. Chen, S. Wang, Y. Liu, A. Baltuska, C. Jin, C. Tian, Z. Tao, *Light Sci. Appl.* **2021**, *10*, 53.
[28] B. Zhu, Z. Fu, Y. Chen, S. Peng, C. Jin, G. Fan, S. Zhang, S. Wang, H. Ru, C. Tian, Y. Wang, H. Kapteyn, M. Murnane, Z. Tao, *Opt. Express* **2022**, *30*, 2918.
[29] J. Guo, Z. Gao, D. Sun, X. Du, Y. Gao, X. Liang, *High Power Laser Sci. Eng.* **2022**, *10*, 10.
[30] J. Schulte, T. Sartorius, J. Weitenberg, A. Vernaleken, P. Russbueldt, *Opt. Lett.* **2016**, *41*, 4511.
[31] M. Hanna, F. Guichard, N. Daher, Q. Bournet, X. Delen, P. Georges, *Laser Photonics Rev.* **2021**, *15*, 2100220.
[32] A. Viotti, M. Seidel, E. Escoto, S. Rajhans, W. Leemans, I. Hartl, C. Heyl, *Optica* **2022**, *9*, 197.
[33] S. Goncharov, K. Fritsch, O. Pronin, *Opt. Lett.* **2023**, *48*, 147.
[34] L. Lavenu, M. Natile, F. Guichard, X. Delen, M. Hanna, Y. Zaouter, P. Georges, *Opt. Express* **2019**, *27*, 1958.
[35] A. Viotti, C. Li, G. Arisholm, L. Winkelmann, I. Hartl, C. Heyl, M. Seidel, *Opt. Lett.* **2023**, *48*, 984.
[36] A. Brodeur, S. L. Chin, *Phys. Rev. Lett.* **1998**, *80*, 4406.
[37] S. Minardi, C. Millian, D. Majus, A. Gopal, G. Tamosauskas, A. Couairon, T. Pertsch, A. Dubietis, *Appl. Phys. Lett.* **2014**, *105*, 224104.
[38] I. Dey, K. Jana, V. Fedorov, A. Koulouklidis, A. Mondal, M. Shaikh, D. Sarkar, L. Amit, S. Tzortzakis, A. Couairon, *Nat. Commun.* **2017**, *8*, 1184.
[39] A. Tcypkin, S. Putilin, M. Melnik, E. Makarov, V. Bespalov, S. Kozlov, *Appl. Opt.* **2016**, *55*, 8390.
[40] J. Stephen, C. Arachchige, T. Hammond, *J. Phys. B: At., Mol. Opt. Phys.* **2022**, *55*, 155402.
[41] W. Liu, S. Petit, N. Zbek, C. Bowden, S. Chin, *Opt. Commun.* **2002**, *202*, 189.
[42] E. Yiwen, L. Zhang, A. Tsypkin, S. Kozlov, C. Zhang, X. Zhang, *J. Opt. Soc. Am. B* **2022**, *39*, 43.
[43] G. Hale, M. Querry, *Appl. Opt.* **1973**, *12*, 555.
[44] E. Yiwen, L. Zhang, A. Tcypkin, S. Kozlov, C. Zhang, X. Zhang, *Ultrafast Sci.* **2021**, *2021*, 9892763.
[45] M. Nisoli, S. Silvestri, O. Svelto, *Appl. Phys. Lett.* **1996**, *68*, 2793.
[46] G. Yang, Y. Shen, *Opt. Lett.* **1984**, *9*, 510.
[47] P. Ho, R. R. Alfano, *Phys. Rev. A* **1979**, *20*, 2170.
[48] L. Bergé, S. Skupin, R. Nuter, J. Kasparian, J. Wolf, *Rep. Prog. Phys.* **2007**, *70*, 1633.
[49] A. Shaykin, V. Ginzburg, I. Yakovlev, A. Kochetkov, A. Kuzmin, S. Mironov, I. Shaikin, S. Stukachev, V. Lozhkarev, A. Prokhorov, E. Khazanov, *High Power Laser Sci. Eng.* **2021**, *9*, e54.
[50] L. He, J. Hu, S. Sun, Y. He, Y. Deng, P. Lan, P. Lu, *J. Phys. B: At., Mol. Opt. Phys.* **2022**, *55*, 205601.